Technical Note

Point-of-use nanobiosensor for detection of dengue virus NS1 antigen in adult *Aedes aegypti*: A potential tool for improved dengue surveillance

Daniel Aaron Wasik, Ashok Mulchandani, and Marylynn V. Yates

Anal. Chem., **Just Accepted Manuscript** • DOI: 10.1021/acs.analchem.7b03407 • Publication Date (Web): 28 Nov 2017

Point-of-use Nanobiosensor for Detection of Dengue Virus NS1 Antigen in Adult *Aedes Aegypti*: A Potential Tool for Improved Dengue Surveillance

Daniel Wasik[a], Ashok Mulchandani[b,c,*], Marylynn V. Yates[a]

[a] *Department of Environmental Sciences, University of California, Riverside*
[b] *Department of Chemical and Environmental Engineering, University of California, Riverside*
[c] *Materials Science and Engineering Program, University of California, Riverside*

Abstract

Dengue virus (DENV) and its primary mosquito vectors *Aedes* spp., have spread to every continent except Antarctica, causing outbreaks and autochthonous transmission in previously disease-free regions. Recently, the spread of other arboviruses carried by invasive *Aedes* spp., such as Chikungunya and Zika, seem to be following similar trends as DENV and have renewed interest in monitoring and modelling arboviruses within mosquito vectors. Unfortunately, current commercially available detection methods are designed for the diagnosis of DENV in humans or are too expensive and complex for sustainable monitoring. We report a novel electronic nanobiosensor utilizing a single-walled carbon nanotube networks chemiresistor transducer functionalized with anti-dengue NS1 monoclonal antibodies for rapid detection of the dengue nonstructural protein 1 (NS1). NS1 is a highly conserved protein secreted at high concentrations during viral replication and is a biomarker for DENV infection. NS1 was successfully detected in spiked adult *Aedes aegypti* homogenate over a broad dynamic range with high sensitivity and selectivity. The biosensor is compatible with "gold-standard" adult mosquito field-collection protocols and generates electronic data that can be readily stored or wirelessly transmitted. Thus, it has potential for remote and real-time monitoring of wild mosquito populations.

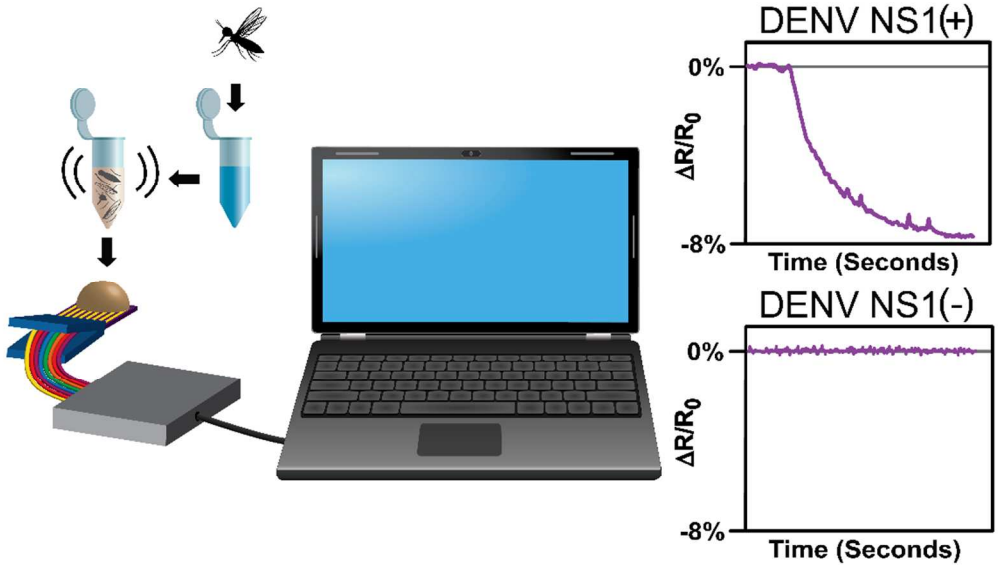

Keywords:
Dengue NS1; Label-free biosensor; Immunosensor; Carbon nanotubes; Aedes Mosquitos
This research was supported by funding from the UCR AES (Agricultural Experiment Station), USDA Hatch Grant (CA-R-ENS-7772-H) and National Science Foundation (1606181). Supporting information available: materials and methods for fabrication of microelectrodes and Figures S1-3.

Introduction

Dengue virus (DENV) has one of the most severe global health burdens of any arthropod-borne disease and is a leading cause of death and disease in endemic nations, especially in poor communities and among children. DENV has long been associated with tropical and subtropical regions. However, global warming, population growth, and other human activities have resulted in habitat expansion for the primary arboviral vectors, *Aedes aegypti* and *Aedes albopictus*, causing a 30-fold increase in the incidence of dengue infections since 1970.[1-4] Unfortunately, habitat modeling predicts further expansion of the habitat range.[5-7] Similarly, West Nile, Chikungunya, and Zika viruses have emerged as global threats and have spread to every inhabited continent causing explosive and unprecedented outbreaks.[8-11] Importantly, these viruses have similar epidemiology, transmission cycle, and diffusion patterns as DENV.[12] Understanding the transmission cycle and sylvatic maintenance of DENV will be key in understanding transmission of these diseases.

Sylvatic DENV amplifications can result in the introduction of a sylvatic strain into the human cycle and outbreaks in urban environments.[13,14] With large populations of asymptomatic humans, relying on hospitalized patients underestimates the incidence and prevalence in the human cycle. Thus, monitoring the diffusion of DENV in mosquito populations is an effective and efficient method for simultaneous monitoring of the disease in both cycles. Early detection of an arbovirus amplification event gives time for medical personnel and government agencies to prepare for a potential outbreak and implement disease prevention and control protocols.[15,16]

Despite its importance, relatively few detection methods are being used to monitor the spread of the disease through vector populations. Commonly, DENV surveillance is performed by field collection of adult mosquitoes with aspirators or box traps followed by detection of DENV with costly and complex laboratory-based methods, such as culturing and PCR.[17,18] Unfortunately, these detection techniques are impractical for large-scale vector surveillance, especially in resource-limited countries. Researchers have proposed using cheaper rapid diagnostic tests (RDT) that target the dengue nonstructural protein 1 (NS1) as a biomarker for infection for vector surveillance.[19-21] NS1 is a highly conserved 46-kDa protein secreted at high concentrations during viral replication in virtually every host organism.[22] However, commercial RDTs have limitations in field surveillance because these devices rely on the user for optical detection, thus compromising the sensitivity and limit of detection.

Thus, new sensing technologies that can assist in rapid assessment of transmission risk and facilitate vector surveillance of DENV infected mosquitoes are urgently needed. Electronic biosensors/immunosensors with single-walled carbon nanotube (SWNT) transducers are rapidly emerging as facile, field-deployable, and cost-effective analytical devices with exquisite sensitivity for transducing antibody-analyte binding events into a measurable electric signal without any label. SWNT's 1-D nanostructure, combined with all surface carbon atoms, enables binding of a large fraction of analyte molecules and modulation of charge carriers in the 'bulk" of the nanometer diameter to produce a large electrical resistance/conductance change.[23] Thus, even low concentrations of analyte can generate significant changes in resistance to produce electronic signal/response that can then be stored and/or wirelessly transmitted. The flexibility of the SWNT platform allows for the use of different bioreceptor elements for the detection of other target analytes, including arboviruses.[24] Additionally, they offer a reliable, rapid, inexpensive, and sensitive diagnostic method that is easily accessible by untrained personnel.[25,26]

Here we report a novel label-free chemiresistor immunosensor for the detection and quantification of dengue NS1 in adult mosquito homogenate that is compatible with "gold-standard" field-collection techniques such the BG-Sentinel and CDC Backpack Aspirator. A network of SWNTs was self-assembled onto lithographically patterned interdigitated gold microelectrodes and functionalized with anti-dengue NS1 monoclonal antibodies. The developed immunosensor had high sensitivity and specificity in both phosphate buffer and mosquito homogenate.

Materials and Methods

Adult *Aedes aegypti* Homogenate

Uninfected adult female *Aedes aegypti* were homogenized using a modified technique common to DENV/NS1 detection.[17,20,27-29] A single adult female *A. aegypti* mosquito was placed into a 2-mL microcentrifuge tube containing 1 mL of 10 mM phosphate buffer, pH 7.2 (PB) and two 5-mm glass beads. The microcentrifuge tube was vortex mixed until homogenization was achieved and care was used to avoid extracting visible debris during aliquot extraction.

Preparation of Anti-Dengue Virus NS1 Glycoprotein Antibody and NS1 Glycoprotein

Mouse monoclonal anti-dengue virus NS1 glycoprotein antibodies (ab138696, Abcam) were buffer exchanged into PB with Micro Bio-Spin P-6 Gel Columns in 10 mM Tris–HCl buffer, pH 7.4 (732-6222, Bio-Rad) according to the manufacturer's instructions. The final antibody concentration after buffer exchange was 240 µg/mL. The full-length DENV NS1 glycoprotein (ab64456, Abcam) was similarly buffer exchanged to a final concentration of 0.1 mg/mL.

Immunosensor Fabrication

Microelectrode fabrication and self-assembly of SWNT networks were performed according to a previously reported method (See Supplementary).[24,30] A 3:1 molar ratio of 1-Pyrenebutyric acid (Sigma Aldrich, USA) and 1-Pyrenebutyric acid N-hydroxysuccinimide ester (Sigma-Aldrich, USA) was mixed into 1 mL of dimethylformamide (DMF). This mixture was incubated on the SWNT networks for 1 h under high humidity for the non-covalent attachment of the pyrene moieties to the SWNT by π-π stacking while leaving the N-hydroxysuccinimide ester available to form an amide bond with anti-NS1 antibody.[31,32] Devices were washed with DMF and dried with N_2 gas. Further incubation steps occurred in the dark at 4 °C, in high humidity environment. Ten µL of buffer-exchanged antibody was incubated on the device for 2 h followed by gentle washing with PB. Next, the devices were incubated successively with 0.1 mM ethanolamine (Sigma-Aldrich, USA) for 15 min to neutralize unreacted N-hydroxysuccinimide ester, 0.1% Tween 20 (BIO-RAD, USA) for 1 h to block any uncoated sites on SWNTs to prevent any non-specific adsorption, and 1% bovine serum albumin (BSA) for 1 h, with gentle washing with PB after each incubation step.

Detection of the NS1 Protein

Immunosensor resistance was monitored in real-time to measure response to different concentrations of NS1 protein in aqueous solutions. Measurements were performed at a fixed source-drain potential (V_{DS}) of 0.1 V, in the dark at room temperature, with humidity modulated by petri dish containing DI water. A single chip has five independent immunosensors/biosensors, each with a single sensing region. Resistance over time was measured by sequentially measuring the resistance for each immunosensor, one at a time, with the sequence restarting approximately every 3 s using a Keithley 2636 digital

multimeter controlled by Arduino Mega 2560 with a LabVIEW interface. The five sensing regions were covered by a single 20-µL drop of PB and allowed to equilibrate. As a control, 10 µL PB was then gently added into the PB drop and immunosensors with ≥ ±5% response to this PB addition were excluded from sensing. Next, 10 µL of NS1-spiked PB were added into the PB drop without washing or further stirring/mixing. The resistance was monitored in real-time and allowed to equilibrate. Once resistance equilibrated, the next 10 µL of a 10-fold higher concentration of NS1-spiked PB was added into the PB drop, repeating until highest concentration was reached. Analysis of mosquito homogenate (MH) followed this protocol with a slight modification. After the initial 10 µL PB control, two additions of 10 µL MH without NS1 were added into the PB drop with equilibration between each addition. Reported NS1 concentrations are adjusted for the increasing volume caused by sample additions. To normalize the measurements, the resistance over time measurement for each individual immunosensor was averaged over 30-s intervals and the percent resistance changes were calculated using the equation

$$[(R_1 - R_0)*100/R_0] \quad (1)$$

where, R_1 is the equilibrated resistance of the immunosensor after each addition and R_0 is the equilibrated resistance of the initial 10-µL PB control addition.

Results and Discussion

As shown in Figure S1, a decrease in current occurs after functionalization with anti-dengue NS1 antibodies, ethanolamine/Tween 20/BSA. The decrease is consistent with literature and attributed to immobilization of fabrication components onto semiconducting p-type SWNT; π–π stacking of the pyrene moieties onto SWNT and/or electron donation and scattering potential of the components.[24,30,33]

Figure 1 shows a representative dynamic/real-time response trace of normalized resistance change (derived from the raw resistance values shown in Fig. S2 using equation 1) for a single immunosensor to increasing concentrations of NS1-spiked PB. Each immunosensor produced a similar observable response (normalized resistance change) upon each addition that reached a plateau (data not shown). These responses were aggregated and averaged over multiple biosensors (*n*) across chips to generate a calibration curve. Following the final NS1 detection, 10 µL of PB was added into the sample, resulting in a negligible average response (-0.66±0.40%). The positive control experiment, in which immunosensors with anti-NS1 antibody were exposed to BSA spiked PB (Figure 2), exhibited minimal response to even high concentrations of BSA protein confirming the decrease in resistance was due specific antibody-NS1 interaction and not due to non-specific interaction/binding of proteins. Additionally, the negative control experiment, in which SWNT networks without anti-NS1 antibody were exposed to NS1 spiked PB (Figure 2), had a minimal response that was not significantly different from the positive control (n=8, $p>0.05$), confirming NS1 is captured by the antibody (Figure 2). Figure 2 illustrates the calibration plot of the averaged plateau responses of the immunosensors as a function of the logarithm of NS1 concentration. When exposed to 0.03 ng/mL, the immunosensors registered a relative resistance change significantly different from the PB blank as well as both controls with comparable protein concentrations (Figure 2, n=12, $p<0.01$). The immunosensors exhibited a sigmoidal calibration plot that was linear between 0.03 ng/mL and $1.39\text{x}10^2$ ng/mL ($y = -7.47x - 59.19$, R^2=0.999; n =12) with a sensitivity (slope) of -7.47±0.14% per log ng/mL. The limit of detection of the immunosensors for NS1 in PB based on a signal to noise (S/N) of 3 was estimated to be 0.09 ng/mL.

In order to simulate field collection, uninfected *A. aegypti* mosquitos were reared in the Insectary and Quarantine Facility at the University of California, Riverside where they were trapped via aspiration, frozen at -20 °C, and sexed. For analysis of mosquito homogenate (MH), multiple 10-µL MH aliquots were first added to the 20-µL drop of PB placed on the sensor. It was determined that two additions were required to blank the immunosensors; further additions of MH resulted in an insignificant response with an average normalized resistance change of -0.22±0.21% per addition, further demonstrating that biosensor response is not due to nonspecific protein interactions (data not shown).

Similar to NS1 spiked PB, the real-time response trace (Figure 3) of a single immunosensor produced an observable response upon each addition of NS1 spiked MH. When SWNT networks without antibody (negative control) were used for sample analysis, the normalized resistance changed on average by -0.6±0.07% per addition of NS1 spiked MH (Figure 4). The normalized resistance change of the MH calibration plot was significantly different from MH controls at each concentration (Figure 4, n=12, $p<0.01$) and was a function of the logarithm of NS1 concentration, which was linear between 0.02 ng/mL and 1.23 x 10^2 ng/mL with a sensitivity (slope) of -7.71 ± 0.2% per log ng/mL ($y = -7.71x - 63.96$, R^2=0.998). The limit of detection of the immunosensors for NS1 in MH for an S/N=3 was estimated to be 0.04 ng/mL. The analytical characteristics of the immunosensors response to NS1 were nearly identical in sensitivity and linear dynamic range in both PB and MH with an insignificant difference (n=12; $p>0.05$) at all NS1 concentrations when Min-Max normalized (Figure S3). Within the working range, intra-chip (3 chips per solution with 4 immunosensors per chip) measurements had a RSD (%) from 2.8 to 13.2 across both PB and MH. The inter-chip (3 chips per solution with 4 immunosensors per chip) RSD was 16.8 across the working range of the PB and MH. These results indicate an appropriate intra- and inter-chip reproducibility for handmade devices. Both intra- and inter-chip measurements had highest RSD at the lowest NS1 concentration.

Compared to the presented SWNT immunosensor, established detection methods such as ELISA and various commercially available RDTs, which are currently preferred for use in the field, have a higher limit of detection (~10 ng NS1/mL) and take longer to obtain results.[34,35] Furthermore, research on various biosensor technologies for DENV NS1 detection has largely been performed in buffer[36-39] and/or human serum samples,[40-43] not mosquito homogenate. However, when compared to these reported biosensors for NS1 detection in PB or PBS, the 0.03 ng/mL limit of detection of this SWNT immunosensor is one of the lowest (Table 1). Additionally, many of the immunosensors use two antibodies, an enzyme label (such as horseradish peroxidase) for signal generation, and multiple incubation/washing steps; making these protocols too tedious/labor intensive and complex for field deployment by untrained personnel.

Vector surveillance plays a critical role in dengue detection and prevention by acting as an early warning system. Early detection of a sylvatic amplification event coupled with a successful outbreak prevention program is much less costly than eradication or control programs established after an outbreak has occurred. Few, if any, biosensors have been reported for detection of NS1 in the vector mosquitoes. Our nanobiosensor offers a facile, affordable, and label-free method for direct detection of the NS1 protein using electrical detection with a high potential for enhancing existing vector surveillance programs and point-of-use diagnostics. The extremely low detection limit, high sensitivity, and 4-orders of magnitude concentration dynamic range of our biosensor makes it well-suited for detection in field-collected mosquitos.[44,45] The SWNT platform's flexibility allows for the use of different bioreceptor elements for detection of other target analytes such as whole DENV and potentially, other arboviruses.[24] As

monitoring systems improve, modelling and predicting the outbreak of zoonotic diseases becomes increasingly viable.

Acknowledgements

We thank Dr. Peter Atkinson and Michael Han for providing *Ae. aegypti* mosquitoes and Thien-Toan Tran for coding and fabricating the Arduino control unit and the LabVIEW interface. We acknowledge the financial support of UCR AES (Agricultural Experiment Station), USDA Hatch Grant (CA-R-ENS-7772-H) and National Science Foundation (1606181).

Figures

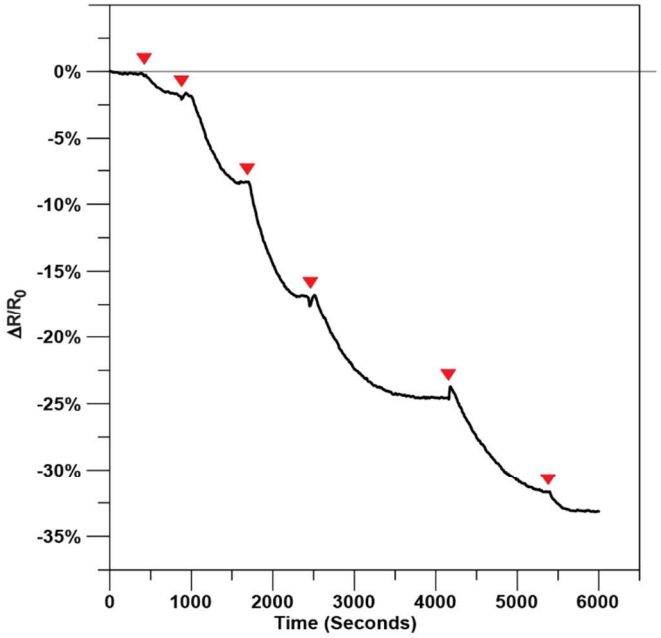

Figure 1. Normalized real-time/dynamic response of a single immunosensor to the addition (▼) of increasing concentrations of NS1 protein in PB from 0.03 ng/mL to $1.23x10^3$ ng/mL.

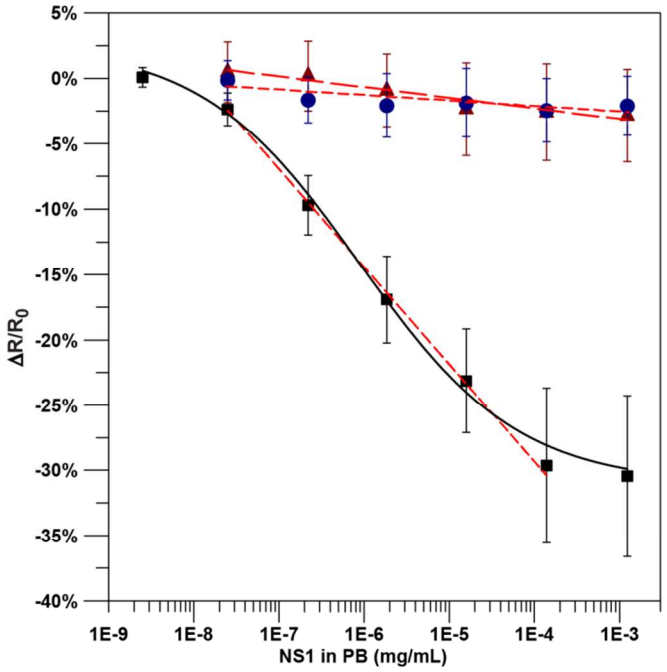

Figure 2. Immunosensor calibration plot: Mean normalized response of immunosensors functionalized with BSA, Tween-20, anti-NS1 antibody to the addition of increasing concentrations of NS1 protein in PB [n=12; y = -7.47x −59.19, R^2=0.999] (■) and to the addition of increasing concentrations BSA protein in PB. [n=9; y = -0.81x −5.57, R^2=0.94] (▲). Mean normalized response of immunosensors functionalized with BSA and Tween-20 but without antibody to the addition of increasing concentrations of NS1 protein in PB [n=8; y = -0.43x −3.89, R^2=0.66] (●). The data points are the mean of the normalized measurements from n independent immunosensors, and error bars represent ±1 standard deviation.

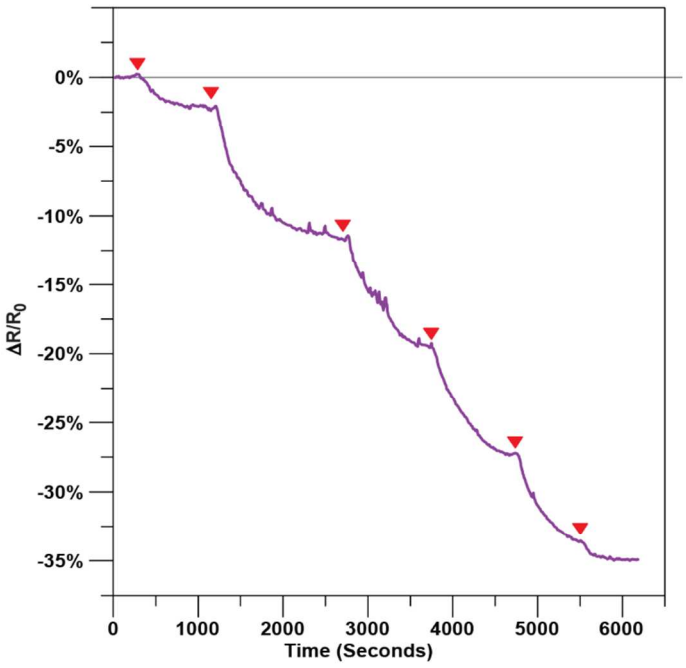

Figure 3. Normalized real-time/dynamic response of a single immunosensor to the addition (▼) of increasing concentrations of NS1 protein in spiked adult *Aedes aegypti* homogenate from 0.02 ng/mL and 1.11 x 10^3 ng/mL.

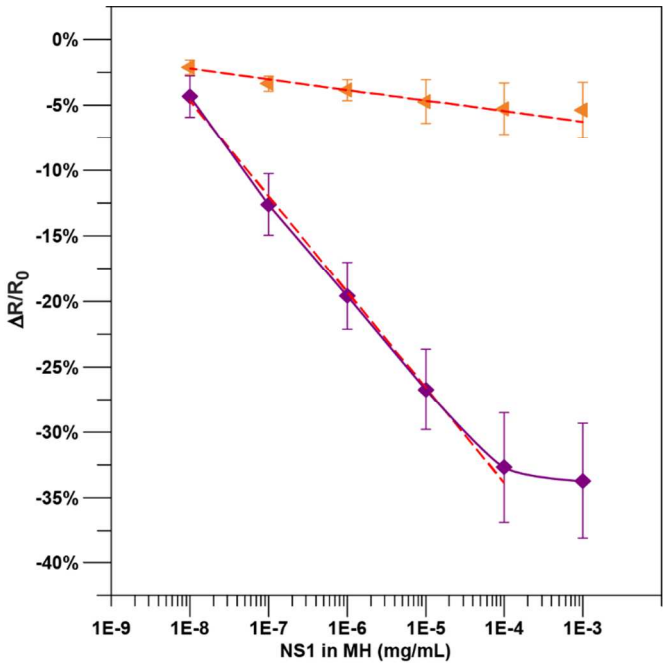

Figure 4. Detection of NS1 in Mosquito Homogenate: Mean normalized response of immunosensors functionalized with BSA, Tween-20, anti-NS1 antibody to the addition of increasing concentrations of NS1 protein in adult *Aedes aegypti* homogenate [n=12; y = -7.71x −63.96, R^2=0.998] (♦). Mean normalized response of immunosensors functionalized with BSA and Tween-20 but without antibody to the addition of increasing concentration*s* of NS1 protein in adult *Aedes aegypti* homogenate [n=5; y = -0.43x –3.89, R^2=0.94] (◄). The data points are the mean of the normalized measurements from *n* independent immunosensors, and error bars represent ±1 standard deviation.

Detection	Method	Range	Sample vol.	Time (min)	LOD	Sensing element	Source
Primary antibody	Chemiresistor Immunosensor	0.03-1200 ng/mL	10 µL	10-20	0.09 ng/mL	Single-walled carbon nanotubes	
Primary antibody	Long range surface plasmon polariton	n/a	20 µL	30-40	5.73 pg/mm^2	Gold stripe embedded in Cytop claddings with an etched microfluidic channel	Wong, et al. [46]
Immobilized anti-NS1 antibodies	Differential pulse voltammetry	1-100 ng/mL	n/a	n/a	0.33 ng/mL	Recordable compact disk chip	Cavalcanti et al., [39]
HRP conjugated secondary antibodies	Electrochemical / amperometric	40-2000 ng/ml	10 µL	30	12 ng/ml	Carbon nanotube-screen printed electrodes	Dias et al., [40]
HRP conjugated secondary antibodies	Electrochemical / amperometric	500-2000 ng/mL	n/a	120	30 ng/mL	Screen printed carbon electrodes	Parkash et al. [47]
Immobilized anti-NS1 antibodies	Quartz crystal microbalance & energy dissipation monitoring	0.01-10 µg/mL	100 µL	10-30	100 ng/ml	Bacterial cellulose nanocrystals	Pirich, et al. [48]
ELISA	ELISA (in serum)	7-284 ng/mL	n/a	3-5 h	7.3 ng/mL	Enzyme immunoassay	Allonso et al., [35]
RDT	Platelia Rapid Diagnostic Assay	n/a	100 µL	140	11.94 ng/mL	One-step sandwich format microplate enzyme immunoassay	Pal, et al. [49]
RDT	Biorad NS1 Ag Strip (in mosquitoes)	n/a	50 µL	15-30	10^6 RNA copies	Immunochromatographic test	Tan et al., [19]
Immobilized anti-NS1 antibodies	Optomagnetic readout	up to 20 µg/mL	6 µL	8	25 ng/mL	Magnetic nanoparticles	Antunes et al., [42]
Immunoelectroactive nanobeads	Electrochemical lateral flow immunosensor	1–25 ng/mL	50 µL	35	0.5 ng/mL	One-step sandwich format microplate enzyme immunoassay	Sinawang et al., [36]
Immobilized anti-NS1 antibodies	Electrochemical impedance spectroscopy	0.01-2.00 µg/mL	50 µL	30	3 ng/ml	Au electrode	Cecchetto et al., [43]
Immobilized IgY anti-NS1 antibodies	Electrochemical impedance spectroscopy	0.1-10 µg/mL	300 µL	5-20	0.09 µg/mL	Disposable Au electrode	Figueiredo et al., [37]
Molecularly imprinted polymers	Quartz crystal microbalance	5-50000 ng/ml	100 µL	5+	n/a	Molecularly imprinted polymers	Tai et al., [38]
HRP conjugated secondary antibodies	Electrochemical / amperometric	0.1-2.5 µg/mL	10 µL	30	0.035 µg/mL	Multi-walled carbon nanotubes	Silva et al., [41]
Fluorescent dyes conjugated to antibody coated polystyrene beads	Spectrofluorometric / ELISA	2- 500 ng/mL	4 µL	45-60	5.2 ng/mL	Sandwich fluorescent immunolinked sorbent assay	Linares, et al. [50]
FITC-tagged secondary antibodies	Fluorescent microscopy	0.05-1000 ng/mL	5 µL	n/a	50 pg/ml	Micro-Spot with integrated pillars	Gunda, et al. [51]
Immobilized anti-NS1 antibodies	Localized surface plasmon resonance	n/a	n/a	30-60	0.074 µg/ml	AuNPs deposited on the endface of a standard multimode fiber	Camara, et al. [52]

Table 1. Comparison of Dengue NS1 detection methods

References

(1) Simmons, C. P.; Farrar, J. J.; Nguyen v, V.; Wills, B. *N Engl J Med* **2012**, *366*, 1423-1432.

(2) Gubler, D. J. *Trop Med Health* **2011**, *39*, 3-11.

(3) Ramasamy, R.; Surendran, S. N. *J Vector Borne Dis* **2016**, *53*, 91-98.

(4) Bai, L.; Morton, L. C.; Liu, Q. *Global Health* **2013**, *9*, 10.

(5) Anker, M. In *Corval C(Eds):*; World Health Organization: Geneva, 2004.

(6) Bonizzoni, M.; Gasperi, G.; Chen, X.; James, A. A. *Trends Parasitol* **2013**, *29*, 460-468.

(7) Gubler, D. J. *Asia Pac J Mol Biol Biotechnol* **2011**, *3*, 111-114.

(8) Weaver, S. C.; Lecuit, M. *N Engl J Med* **2015**, *372*, 1231-1239.

(9) Berthet, N.; Nakouné, E.; Kamgang, B.; Selekon, B.; Descorps-Declère, S.; Gessain, A.; Manuguerra, J.-C.; Kazanji, M. *Vector Borne Zoonotic Dis* **2014**, *14*, 862-865.

(10) Diallo, D.; Sall, A. A.; Buenemann, M.; Chen, R.; Faye, O.; Diagne, C. T.; Faye, O.; Ba, Y.; Dia, I.; Watts, D.; Weaver, S. C.; Hanley, K. A.; Diallo, M. *PLoS Negl Trop Dis* **2012**, *6*, e1649.

(11) Petersen, L. R.; Brault, A. C.; Nasci, R. S. *JAMA* **2013**, *310*, 308-315.

(12) Musso, D.; Cao-Lormeau, V. M.; Gubler, D. J. *Lancet* **2015**, *386*, 243-244.

(13) Althouse, B. M.; Lessler, J.; Sall, A. A.; Diallo, M.; Hanley, K. A.; Watts, D. M.; Weaver, S. C.; Cummings, D. A. *PLoS Negl Trop Dis* **2012**, *6*, e1928.

(14) Durbin, A. P.; Mayer, S. V.; Rossi, S. L.; Amaya-Larios, I. Y.; Ramos-Castaneda, J.; Eong Ooi, E.; Jane Cardosa, M.; Munoz-Jordan, J. L.; Tesh, R. B.; Messer, W. B.; Weaver, S. C.; Vasilakis, N. *Virology* **2013**, *439*, 34-41.

(15) Centers for Disease, C.; Prevention. *MMWR Morb Mortal Wkly Rep* **2001**, *50*, 57-59.

(16) Sharp, T. M.; Moreira, R.; Soares, M. J.; Miguel da Costa, L.; Mann, J.; DeLorey, M.; Hunsperger, E.; Muñoz-Jordán, J. L.; Colón, C.; Margolis, H. S.; de Caravalho, A.; Tomashek, K. M. *Emerg Infect Dis* **2015**, *21*, 1311-1316.

(17) Ritchie, S. A.; Buhagiar, T. S.; Townsend, M.; Hoffmann, A.; Van Den Hurk, A. F.; McMahon, J. L.; Eiras, A. E. *J Med Entomol* **2014**, *51*, 210-219.

(18) Frentiu, F. D.; Zakir, T.; Walker, T.; Popovici, J.; Pyke, A. T.; van den Hurk, A.; McGraw, E. A.; O'Neill, S. L. *PLoS Negl Trop Dis* **2014**, *8*, e2688.

(19) Tan, C.-H.; Wong, P.-S.; Li, M.-Z.; Vythilingam, I.; Ng, L.-C. *Vector Borne Zoonotic Dis* **2011**, *11*, 789-792.

(20) Voge, N. V.; Sánchez-Vargas, I.; Blair, C. D.; Eisen, L.; Beaty, B. J. *Am J Trop Med Hyg* **2013**, *88*, 260-266.

(21) Sylvestre, G.; Gandini, M.; de Araújo, J. M.; Kubelka, C. F.; Lourenço-de-Oliveira, R.; Maciel-de-Freitas, R. *Parasit Vectors* **2014**, *7*, 155.

(22) Winkler, G.; Maxwell, S. E.; Ruemmler, C.; Stollar, V. *Virology* **1989**, *171*, 302-305.

(23) Chartuprayoon, N.; Zhang, M.; Bosze, W.; Choa, Y. H.; Myung, N. V. *Biosens Bioelectron* **2015**, *63*, 432-443.

(24) Wasik, D.; Mulchandani, A.; Yates, M. V. *Biosens Bioelectron* **2017**, *91*, 811-816.

(25) Ramnani, P.; Saucedo, N. M.; Mulchandani, A. *Chemosphere* **2016**, *143*, 85-98.

(26) García-Aljaro, C.; Cella, L. N.; Shirale, D. J.; Park, M.; Muñoz, F. J.; Yates, M. V.; Mulchandani, A. *Biosens Bioelectron* **2010**, *26*, 1437-1441.

(27) Muller, D. A.; Frentiu, F. D.; Rojas, A.; Moreira, L. A.; O'Neill, S. L.; Young, P. R. *J Virol Methods* **2012**, *183*, 90-93.

(28) Armstrong, P. M.; Andreadis, T. G.; Finan, S. L.; Shepard, J. J.; Thomas, M. C. *Journal of Visualized Experiments* **2011**, 2889.

(29) Duong, V.; Lambrechts, L.; Paul, R. E.; Ly, S.; Lay, R. S.; Long, K. C.; Huy, R.; Tarantola, A.; Scott, T. W.; Sakuntabhai, A.; Buchy, P. *Proc Natl Acad Sci U S A* **2015**, *112*, 14688-14693.

(30) Ramnani, P.; Gao, Y.; Ozsoz, M.; Mulchandani, A. *Anal Chem* **2013**, *85*, 8061-8064.

(31) Stefansson, S.; Kwon, H. H.; Ahn, S. N. *J. Nanotechnol.* **2012**, *2012*, 1-8.

(32) Kim, J. P.; Lee, B. Y.; Lee, J.; Hong, S.; Sim, S. J. *Biosens Bioelectron* **2009**, *24*, 3372-3378.

(33) Gruner, G. *Anal Bioanal Chem* **2006**, *384*, 322-335.

(34) Young, P. R.; Hilditch, P. A.; Bletchly, C.; Halloran, W. *J Clin Microbiol* **2000**, *38*, 1053-1057.

(35) Allonso, D.; Meneses, M. D.; Fernandes, C. A.; Ferreira, D. F.; Mohana-Borges, R. *PLoS ONE* **2014**, *9*, e113634.

(36) Sinawang, P. D.; Rai, V.; Ionescu, R. E.; Marks, R. S. *Biosens Bioelectron* **2016**, *77*, 400-408.

(37) Figueiredo, A.; Vieira, N. C.; dos Santos, J. F.; Janegitz, B. C.; Aoki, S. M.; Junior, P. P.; Lovato, R. L.; Nogueira, M. L.; Zucolotto, V.; Guimarães, F. E. *Sci Rep* **2015**, *5*, 7865.

(38) Tai, D.-F.; Lin, C.-Y.; Wu, T.-Z.; Chen, L.-K. *Anal Chem* **2005**, *77*, 5140-5143.

(39) Cavalcanti, I. T.; Guedes, M. I. F.; Sotomayor, M. D. P. T.; Yamanaka, H.; Dutra, R. F. *Biochem Eng J* **2012**, *67*, 225-230.

(40) Dias, A. C.; Gomes-Filho, S. L.; Silva, M. M.; Dutra, R. F. *Biosens Bioelectron* **2013**, *44*, 216-221.

(41) Silva, M. M. S.; Dias, A. C. M. S.; Silva, B. V. M.; Gomes-Filho, S. L. R.; Kubota, L. T.; Goulart, M. O. F.; Dutra, R. F. *J Chem Technol Biot* **2015**, *90*, 194-200.

(42) Antunes, P.; Watterson, D.; Parmvi, M.; Burger, R.; Boisen, A.; Young, P.; Cooper, M. A.; Hansen, M. F.; Ranzoni, A.; Donolato, M. *Sci Rep* **2015**, *5*, 16145.

(43) Cecchetto, J.; Carvalho, F. C.; Santos, A.; Fernandes, F. C. B.; Bueno, P. R. *Sensor Actuat B-Chem* **2015**, *213*, 150-154.

(44) Anderson, J. R.; Rico-Hesse, R. *Am J Trop Med Hyg* **2006**, *75*, 886-892.

(45) Bennett, K. E.; Olson, K. E.; Muñoz, M. D.; Fernandez-Salas, I.; Farfan-Ale, J. A.; Higgs, S.; Black, W. C.; Beaty, B. J. *Am J Trop Med Hyg* **2002**, *67*, 85-92.

(46) Wong, W. R.; Sekaran, S. D.; Adikan, F. R.; Berini, P. *Biosens Bioelectron* **2016**, *78*, 132-139.

(47) Parkash, O.; Yean, C. Y.; Shueb, R. H. *Diagnostics (Basel)* **2014**, *4*, 165-180.

(48) Pirich, C. L.; de Freitas, R. A.; Torresi, R. M.; Picheth, G. F.; Sierakowski, M. R. *Biosens Bioelectron* **2017**, *92*, 47-53.

(49) Pal, S.; Dauner, A. L.; Mitra, I.; Forshey, B. M.; Garcia, P.; Morrison, A. C.; Halsey, E. S.; Kochel, T. J.; Wu, S.-J. *PLoS ONE* **2014**, *9*, e113411.

(50) Linares, E. M.; Pannuti, C. S.; Kubota, L. T.; Thalhammer, S. *Biosens Bioelectron* **2013**, *41*, 180-185.

(51) Gunda, N. S.; Singh, M.; Purwar, Y.; Shah, S. L.; Kaur, K.; Mitra, S. K. *Biomed Microdevices* **2013**, *15*, 959-971.

(52) Camara, A. R.; Gouvêa, P. M.; Dias, A. C.; Braga, A. M.; Dutra, R. F.; de Araujo, R. E.; Carvalho, I. C. *Opt Express* **2013**, *21*, 27023-27031.